CHIN. PHYS. LETT. Vol. 29, No. 4 (2012) 046802

Solid Phase Reactions of Ni-GaAs Alloys for High Mobility Ⅲ–V MOSFET Applications *

LU Li(卢力), CHANG Hu-Dong(常虎东), SUN Bing(孙兵), WANG Hong(王虹), XUE Bai-Qing(薛百清), ZHAO Wei(赵威), LIU Hong-Gang(刘洪刚)**

Microwave Device and IC Department, Institute of Microelectronics, Chinese Academy of Sciences, Beijing 100029

(Received 13 December 2011)

The solid phase reactions of Ni with GaAs substrates are investigated. The experimental results reveal that the Ni-GaAs solid phase reaction forms a ternary phase of Ni_2GaAs when annealing temperatures are in the range 250–300°C. As the annealing temperature increases to 400°C, the Ni_2GaAs phase starts to decompose due to NiAs phase precipitation. Ni-GaAs alloys processed at 400°C with a 3 min annealing time demonstrate a sheet resistance of 30 Ω/square after unreacted Ni removal in hot diluted-HCl solutions. Therefore, Ni-GaAs alloys formed by solid phase reaction could be promising metallic source/drain structures with significant low series resistance for high mobility Ⅲ–V metal-oxide-semiconductor field effect transistor (MOSFET) applications.

PACS: 68.35.Ct, 73.61.Ey, 85.30.Tv DOI: 10.1088/0256-307X/29/4/046802

Ⅲ–V-based metal-oxide-semiconductor field effect transistors (MOSFETs) offer great advantages over silicon MOSFETs for both high speed and radio frequency applications due to the higher electron mobility, higher breakdown field, as well as the availability of semi-insulating substrates.[1–9] One of the critical challenges for Ⅲ–V MOSFETs is the high series resistance of the source/drain (S/D), which significantly limits the drain current density owing to the low doping solubility in Ⅲ–V compound semiconductors.[3–6] To realize low S/D series resistance in Ⅲ–V MOSFETs, a self-aligned metallic S/D structure is believed to be a promising alternative.[5–9]

The Ni-GaAs alloy reaction was widely studied because Ni works as a conglutination layer in conventional GaAs-Ni/Ge/Au ohmic contacts.[10–15] Researchers found that Ni was the predominant diffusion species and a ternary-phase Ni_xGaAs ($x = 2.5$–4) was formed in the range 200–300℃.[16] Lahav *et al.*[14] described a detailed reaction process where Ni-GaAs (001) produced Ni_2GaAs at 250℃, then precipitated the NiAs phase in the range 350–550℃, eventually turning into NiGa and NiAs phases as the temperature exceeded 600℃. However, unlike the nickel-silicide process, the solid phase reactions between nickel and GaAs materials for the formation of Ni-GaAs S/D alloys, which have a low sheet resistance and a high etching selectivity against nickel films, have not yet been studied. In this Letter, Ni-GaAs solid phase reactions at various thermal annealing conditions are systematically studied. The circular transmission line model (CTLM), Raman spectra and scanning electron microscopy (SEM) are used to characterize the sheet resistance R_{sh}, the phase compositions, as well as the microstructures of Ni-GaAs alloys, respectively.

The GaAs samples used for this study were a 4 inch (100) semi-insulating GaAs (SI-GaAs) wafer with a resistivity higher than $1 \times 10^7\ \Omega$·cm, and an n-type GaAs (n-GaAs) epi-wafer with a sheet resistance of 415 Ω/square, consisting of 1000 nm GaAs Si-doped to $\sim 5\times10^{16}\ cm^{-3}$ and 10 nm GaAs Si-doped to $\sim 2\times10^{19}\ cm^{-3}$, sequentially grown on (100) SI-GaAs substrates. The wafers were degreased in acetone and ethanol, respectively, and then etched in a solution ($HCl:H_2O$ = 1:10) for 2 min to remove the native oxide. Finally, the wafers were rinsed in flowing deionized (DI) water, and dried in nitrogen gas. After the surface treatments of the wafers, a 15 nm thick Ni film was deposited onto the cleaned GaAs substrates by e-beam evaporation at a chamber pressure of 10^{-6} Torr. Sequentially, the GaAs wafers were cut into small pieces (1 cm × 1 cm), and then annealed at 250–400℃ in nitrogen ambient by using an AG Associates Mini Pulse rapid thermal annealing (RTA) furnace for 60 s. After the RTA processes, the unreacted Ni films on different samples were dealt with by four methods: (1) 37% hydrochloric acid solution on Ni-GaAs(SI) at room temperature; (2) hot diluted hydrochloric acid ($HCl:H_2O$ = 1:10) solution on Ni-GaAs(SI) at 60℃; (3) as-annealed Ni-GaAs(SI) films; and (4) hot diluted hydrochloric acid ($HCl:H_2O$ = 1:10) solution on Ni-GaAs(n^+) at 60℃. The sheet resistances R_{sh} for the Ni-GaAs(SI) and Ni-GaAs(n^+) alloys were measured by the CTLM method. The composition of the Ni-GaAs alloy was determined by Raman spectra, and the surface morphologies of the Ni-GaAs alloys were inspected by SEM.

Figure 1 shows the R_{sh} of Ni-GaAs(SI) and Ni-GaAs(n^+) annealed at elevated temperatures varying from 250℃ to 400℃ for 1 min. The R_{sh} of the as-annealed Ni-GaAs(SI) sample with the unreacted Ni film increases from 18.8 Ω/square at 250℃ to 32 Ω/square at 400℃, owing to Ni consumption during the Ni-GaAs solid phase reaction, seen in Fig. 1(c). Af-

*Supported by the National Basic Research Program of China under Grant Nos 2011CBA00605 and 2010CB327501, the National Science & Technology Major Project of China under Grant No 2011ZX02708-003, One-Hundred Talent Program of Chinese Academy of Sciences, and the Scientific Research Foundation for the Returned Overseas Chinese Scholars, Ministry of Education of China.

**Corresponding author. Email: liuhonggang@ime.ac.cn

© 2012 Chinese Physical Society and IOP Publishing Ltd

ter 37% HCl and hot diluted HCl treatments, the R_{sh}'s of the samples annealed at 250℃ are 622 Ω/square and 573 Ω/square, respectively, as seen in Figs. 1(a) and 1(b). These significantly high R_{sh}'s indicate that Ni and SI-GaAs films react slightly at 250℃. When the annealing temperature increases to 400℃, the R_{sh}'s of the Ni-GaAs(SI) samples etched by hot diluted-HCl decrease to 37 Ω/square, which means that the Ni film has been reacted with GaAs substrates and the reaction products have good electrical conductivity. On the other hand, the R_{sh} of Ni-GaAs(n^+) decreases with the increase in annealing temperature as Ni-GaAs reactions as well, and reaches a sheet resistance of 32.1 Ω/square, which is almost 1/13 of the n-GaAs epitaxial layer (R_{sh}∼415 Ω/square). The considerable decrement in the sheet resistance of the Ni-GaAs(n^+) alloy indicates that the Ni-GaAs S/D contact process in this work can achieve high performance GaAs MOSFETs. However, for the 37% HCl etched Ni-GaAs(SI) sample annealed at 400℃, R_{sh} is still as high as 161 Ω/square for 37% HCl solution, not only for the etched unreacted Ni film, but also for the partly etched Ni-GaAs alloy. As the Ni-GaAs alloy plays a decisive role in the conductivity of the NiGaAs/GaAs material system[10–12] and the sheet resistances are nearly inverse ratios to the thickness of the conductive films, the sheet resistance increases as a result of the loss of alloy, as seen in Figs. 1(a) and 1(b).

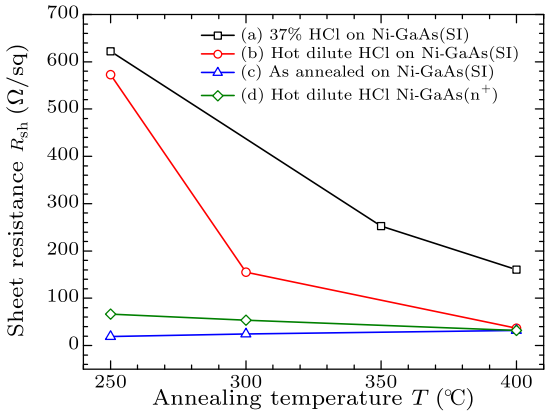

Fig. 1. Sheet resistance measured after annealing 15 nm Ni on GaAs and GaAs(n^+) substrates at various temperatures for 60 s. The sheet resistances of the samples were dealt with by different methods: (a) 37% hydrochloric acid solution on semi-insulating GaAs at room temperature; (b) hot diluted hydrochloric acid ($HCl:H_2O$ = 1:10) solution on semi-insulating GaAs; (c) as-annealed Ni-GaAs films (on semi-insulating GaAs); and (d) hot diluted hydrochloric acid ($HCl:H_2O$ = 1:10) solution on n^+-doping GaAs.

In order to study the dependence of sheet resistance on the annealing time, Ni-GaAs samples were annealed for 60, 120 and 180 s, respectively. As shown in Fig. 2, Ni-GaAs alloys annealed at 400℃ exhibit a much steeper slope. It is possible that the annealing time has an effect not only on the diffusion depth but also on the production of reactions, and both influences are able to change the R_{sh}. However, the compositions of the Ni-GaAs alloy observed by Raman spectra are proved to be constant for various times at 400℃, as seen in Fig. 3(b). The influence of annealing time on the sheet resistance value is based on the fact that there is a linear relationship between the square root of the annealing time ($\sqrt{t}$) and the diffusion-zone length L, as defined in $L \propto \sqrt{t}$.[10–15] Based on the experimental data presented in Fig. 2, a relationship among the R_{sh} of the Ni-GaAs alloy, the annealing temperature and time is proposed as follows:

$$R_{sh} = 0.1735 \times \frac{(t^{-0.5} - 2.75)}{\sqrt{\exp[-1.08 \times 10^4/RT]}} + 9.89, \quad (1)$$

where R and T are the gas constant and annealing temperature, respectively. Moreover, the time t must be more than 0.5 min to ensure the occurrence of the annealing process, and less than 10 min to be compatible to other low-temperature processes.

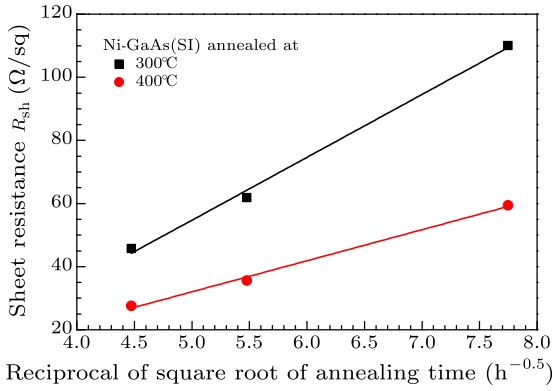

Fig. 2. The dependence of sheet resistance on the square root of the annealing time for 300℃ and 400℃ annealed Ni-GaAs alloys. The annealing times are 60, 120 to 180 s, respectively.

As shown in Fig. 3(a), Raman spectroscopy measurements are used to determine the solid phase compositions of the annealed Ni-GaAs alloy. The broad peak located in the 160.4–226.2 cm^{-1} region corresponds to the NiAs phase, the peak centered at 271.5 cm^{-1} corresponds to the GaAs phase, and the broad peak located in the 509.7–536.9 cm^{-1} region corresponds to the $Ni_{2-x}GaAs_{1-x}$ phase. Compared with the Ni-GaAs alloy annealed at 300℃, the broad peaks located at 160.4–226.2 cm^{-1} and 509.7–536.9 cm^{-1} are more intense,[20–25] which might be attributed to the Ni_2GaAs phase decomposition at 400℃ and the NiAs phase precipitation. Otherwise, because the Ni_2GaAs formed rectifying contacts with a barrier height of 0.84 eV, whereas NiAs shows an ohmic behavior at the interface, it can be proved that the R_{sh} decline at 400℃ results from the Ni_2GaAs decomposition and NiAs phase precipitation, as seen in Figs. 1(a), 1(b) and 1(d). This phenomenon is consistent with the Ni-GaAs solid phase reaction reported by Lahav *et al.*[14] The solid phase reaction is given by

$$Ni_2GaAs \rightarrow Ni_{2-x}GaAs_{1-x} + xNiAs. \quad (2)$$

To further study the dependence of the solid phase reaction on annealing time, the samples were annealed at 400℃ for 1 min, 2 min and 3 min, respectively. As shown in Fig. 3(b), the Raman peak positions and peak intensities have negligible difference, which indicates that 1 min is long enough for Ni_2GaAs phase decomposition and NiAs phase precipitation.

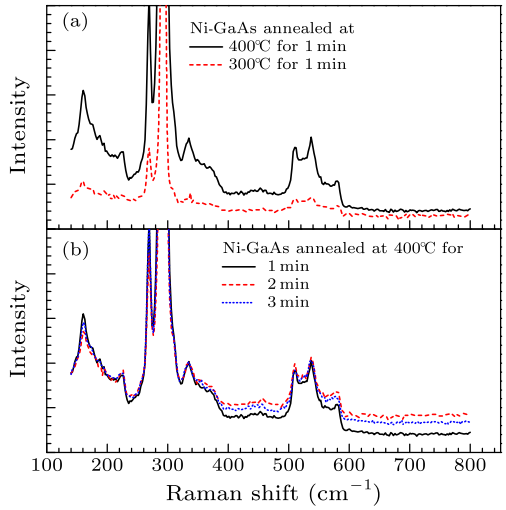

Fig. 3. Raman spectra for Ni-GaAs alloys annealed at 300℃ and 400℃ for 1 min (a), and 300℃ for 1, 2 and 3 min (b).

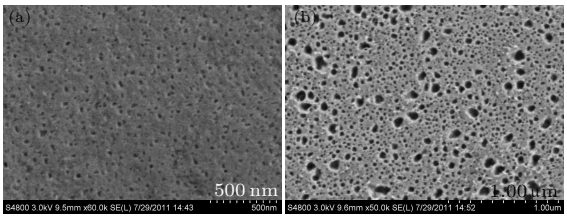

Fig. 4. SEM images of Ni-GaAs alloys annealed at (a) 300℃ and (b) 400℃ for 1 min after Ni removal in diluted HCl for 3 min.

To ascertain the surface morphology of the Ni-GaAs alloy, after unreacted Ni was removed in diluted HCl for 3 min, Ni-GaAs alloys annealed at 300℃ and 400℃ for 60 s were also studied using SEM. As shown in Fig. 4, compared to a decent surface morphology of Ni-GaAs alloy annealed at 300℃, the Ni-GaAs alloy annealed at 400℃ exhibits a more porous surface, which could be attributed to severe phase segregation of Ni_2GaAs and formation of an NiAs phase at high temperature. As a result, the high dissolving rate of the NiAs phase in the hot diluted-HCl solution leads to porous surface morphology. In future research, we will focus on the relationships between annealing, etching conditions and surface morphology.

In conclusion, the solid phase reactions of Ni with semi-insulating GaAs and n-type GaAs have been studied. CTLM, Raman spectra and SEM are used to characterize the sheet resistance, phase compositions, as well as the microstructures of Ni-GaAs alloys formed under various thermal annealing conditions. Ni-GaAs alloys processed at 300℃ for 3 min demonstrate a sheet resistance of about 30 Ω/square and a decent surface morphology after unreacted Ni removal. The measurements reveal the formation of a ternary phase of Ni_2GaAs when Ni and GaAs are annealed at 250–300℃, and the Ni_2GaAs phase starts to decompose due to NiAs phase precipitation when the annealing temperature increases up to 400℃. Low enough R_{sh} values of Ni-GaAs(n^+) and Ni-GaAs(SI) alloys annealed at 300–400℃ show great potential for use as S/D metals for high-mobility GaAs-based Ⅲ–Ⅴ MOSFETs with significant low series resistance, so this needs to be studied further.

References

[1] Xuan Y, Wu Y Q, and Ye P D 2008 *IEEE Electron Device Lett.* **29** 294
[2] Xuan Y, Wu Y Q and Ye P D 2007 *Tech. Dig. Int. Electron Device Meet.* p 637
[3] Huang M L, Chang Y C, Chang C H, Lee Y J, Chang P, Kwo J, Wu T B and Hong M 2005 *Appl. Phys. Lett.* **87** 252104
[4] Datta S, Dewey G, Fastenau J M, Hudait M K, Loubychev D, Liu W K, Radosavljevic M, Rachmady W and Chau R 2007 *IEEE Electron Device Lett.* **8** 28
[5] Kim S H, Yokoyama M, Taoka N, Iida R, Lee S, Nakane R, Urabe Y, Miyata N, Yasuda T, Yamada H, Fukuhara N, Hata M, Takenaka M and Takagi S 2010 *Tech. Dig. Int. Electron Device Meet.* p 596
[6] Kim S H, Yokoyama M, Taoka N, Iida R and Lee S 2011 *Appl. Phys. Express* **4** 024201
[7] Zhang X G, Guo H X, Gong X, Zhou Q, Lin Y R, Lin H Y, Ko C H, Wann C H and Yeo Y C 2011 *Electrochem. Solid State Lett.* **14** H60
[8] Zhang X G, Guo H X, Lin H Y, Ivana, Gong X, Zhou Q, Lin Y R, Ko C H, Wann C H and Yeo Y C 2011 *Electrochem. Solid State Lett.* 14 H212
[9] Yeo Y C, Chin H C, Gong X, Guo H X and Zhang X G 2011 *219th ECS Meeting* p 1217
[10] Shih Y C, Murakami M and Price W H 1989 *J. Appl. Phys.* **65** 3539
[11] Tsunoda Y and Murakami M 2002 *J. Electr. Mater.* 3176
[12] Murakami M, Childs K D, Baker J M and Callegari A 1986 *J. Vac. Sci. Technol.* B **4** 903
[13] Guivarc'h A, Guerin R, Caulet J, Poudoulec A and Fontenille J 1989 *J. Appl. Phys.* **66** 2129
[14] Lahav A, Eizenberg M and Komem Y 1986 *J. Appl. Phys.* **60** 991
[15] Yamaguchi A and Asamizu H 1999 *J. Appl. Phys.* **85** 7792
[16] Waldrop J R and Grant R W 1979 *Appl. Phys. Lett.* **34** 630
[17] Chen S H, Carter C B, Palmstrom C J and Ohashi T 1986 *Appl. Phys. Lett.* **48** 803
[18] Guivarc'h A, Caulet J and Minier M 1994 *J. Appl. Phys.* **75** 5061
[19] Guenna R and Guivarc'h A 1989 *J. Appl. Phys.* **66** 2122
[20] Wuyts J W, Silverans R E, Van H M and Rossum M V 1994 *J. Appl. Phys.* **75** 2055
[21] Rainer S F 1988 *J. Electr. Mater.* **17** 193
[22] Sands T, Keramidas V G, Washburn J and Gronsky R 1986 *Appl. Phys. Lett.* **48** 402
[23] Zhang S L, Gant T A, Delaney M, Klein M V, Klem J and Morkoc H 1988 *Chin. Phys. Lett.* **5** 113
[24] Xiao G M, Yin S D, Zhang J P, Fan T W, Liu J R, Ding A J, Zhou J M and Zhu P R 1989 *Chin. Phys. Lett.* **6** 451
[25] *University of Arizona Mineral Museum*(3636) RRUFF R060121(Nickeline) http://rruff.info/nickel/source/asc/R060121